Physics Letters B 748 (2015) 173–177

Contents lists available at ScienceDirect

Physics Letters B

www.elsevier.com/locate/physletb

Competing particle–hole excitations in ^{30}Na: Constraining state-of-the-art effective interactions

M. Petri [a,*], P. Fallon [b], A.O. Macchiavelli [b], S. Heil [a], E. Rodriguez-Vieitez [b,c], D. Bazin [d], C.M. Campbell [d,e,1], R.M. Clark [b], M. Cromaz [b], A. Gade [d,e], T. Glasmacher [d,e], I.Y. Lee [b], S. Malbrunot-Ettenauer [d,e,2], S. Paschalis [a], A. Ratkiewicz [d,e], J.R. Terry [d,e], D. Weisshaar [d], M. Wiedeking [b,3]

[a] Institut für Kernphysik, Technische Universität Darmstadt, Darmstadt, D 64289, Germany
[b] Nuclear Science Division, Lawrence Berkeley National Laboratory, Berkeley, CA 94720, United States
[c] Department of Nuclear Engineering, University of California, Berkeley, CA 94720, United States
[d] National Superconducting Cyclotron Laboratory, Michigan State University, East Lansing, MI 48824, United States
[e] Department of Physics and Astronomy, Michigan State University, East Lansing, MI 48824, United States

ARTICLE INFO

Article history:
Received 28 May 2015
Accepted 27 June 2015
Available online 2 July 2015
Editor: V. Metag

Keywords:
"Island of Inversion"
Knockout reactions
Radioactive ion beams
Effective interaction
Particle–hole excitations
Negative parity

ABSTRACT

The odd–odd nucleus ^{30}Na is studied via a one-proton, one-proton–one-neutron and one-neutron removal reaction using an intermediate-energy ^{31}Mg, ^{32}Mg and ^{31}Na radioactive ion beam, respectively. Combining high-resolution γ-ray spectroscopy with the selectivity of the three reaction mechanisms, we are able to distinguish multiple particle–hole configurations. Negative-parity states in ^{30}Na are observed for the first time, providing an important measure of the excitation of the 1p1h/3p3h configuration and hence the *sd–pf* shell gap. The extracted band structures and level energies serve as invaluable input for the theoretical refinement of the effective interactions used in this region.

1. Introduction

The nuclear shell structure and the corresponding magic numbers change dramatically as one moves away from the valley of beta stability, see Ref. [1] for a recent review. The breakdown of the $N = 20$ magic number was the first indication of this shell evolution when an excess in the binding energy of ^{31}Na was observed by Thibault et al. [2] in a mass measurement experiment. This was attributed to a deformed ground-state configuration [3–5]. Around ^{31}Na and $N = 20$ a number of other nuclei with the same properties (deformed ground state) have been observed, forming a region of deformed nuclei commonly referred to as the "Island of Inversion"; a collection of examples and references is given in Ref. [1]. In this region, the expected filling of the neutron orbitals (i.e. the $N = 20$ nuclei fully occupying the neutron *sd* shell) is not fulfilled and the ground-state configuration of these nuclei is dominated by the *pf* neutron orbitals. The driving mechanism behind this inversion is the gain in correlation energy as neutrons are promoted from the *sd* to the *pf* shell coupled with a reduced $N = 20$ shell gap, as recently discussed in Refs. [6–9].

For neutron number $N = 20$ and proton numbers Z = 10–12 (e.g. ^{30}Ne, ^{31}Na, ^{32}Mg), the gain in correlation energy by promoting two neutrons in the *pf* shell is large and therefore such intruder configurations become the ground state even in the presence of a relatively large *sd–pf* shell gap [10]. However, for nuclei with $N < 20$ the dominance of intruder configurations becomes less favored, because of the large correlation energy that an open-shell nucleus already gains from the interaction between protons and neutrons at normal states [10]. In the neutron-rich Na isotopic chain, ^{30}Na is of particular interest. The probability of intruder

* Corresponding author.
E-mail address: mpetri@ikp.tu-darmstadt.de (M. Petri).
[1] Nuclear Science Division, Lawrence Berkeley National Laboratory, Berkeley, CA 94720.
[2] CERN, Physics Department, 1211 Genève 23, Switzerland.
[3] iThemba LABS, PO Box 722, Somerset West 7129, South Africa.

http://dx.doi.org/10.1016/j.physletb.2015.06.067

2p2h[4] configurations in the lowest positive-parity state of ^{30}Na, as calculated by Utsuno et al. [10], varies dramatically as a function of the sd–pf shell gap and there is a sharp transition between a "normal" and "intruder" dominated configuration within a small change in the shell gap. This is not the case for ^{29,31}Na, where the transition between normal (0p0h) and intruder (2p2h) configurations is far more gradual. The sensitivity of the structure of this nucleus to the sd–pf shell gap turns ^{30}Na into a key nucleus and motivated this experimental investigation with particular emphasis on negative-parity states, arising from 1p1h and 3p3h excitations, which have not been experimentally observed so far.

The deviation of the low-lying properties of ^{30}Na from the USD predictions was already evident in 1978, when Huber et al. [11] measured a smaller magnetic moment in ^{30}Na than expected. Recent studies of excited states in ^{30}Na include intermediate-energy Coulomb excitation [12,13], proton inelastic scattering [14], a β-decay study [15] and a low-energy Coulomb excitation experiment [16]. All of these studies (except from [12]) agree that the ground state of ^{30}Na contains 2p2h excitations. In these experiments, only a few excited states in ^{30}Na have been observed, most of them in the β-decay experiment; all of them are considered to be of positive parity.

In this paper, we report on the low-lying structure of ^{30}Na, populated by three different nucleon-removal reactions. The one-neutron and one-proton removal reactions proceed as direct reactions and will lead to different final state populations. We have used this feature to associate the observed band structures to specific dominant npnh configurations. Specifically, we identify the key negative parity states for the first time.

2. Experimental details

The experiment was performed at the National Superconducting Cyclotron Laboratory at Michigan State University. ^{30}Na was populated via three nucleon-removal reactions, a one-proton (1p) knockout reaction from a secondary ^{31}Mg beam, a one-proton–one-neutron (1p1n) removal reaction from a secondary ^{32}Mg beam and a one-neutron (1n) knockout reaction from a secondary ^{31}Na beam.[5] These secondary beams were produced by the fragmentation of a 140 MeV/u primary ^{48}Ca beam (delivered from the Coupled Cyclotron Facility) on a thick ^{9}Be production target (888 mg/cm^2). The secondary beams of interest were selected in the A1900 separator [17] and identified on an event-by-event basis through time-of-flight measurements. They were delivered to the experimental hall (S3 Vault) with an energy of 93 MeV/u for ^{31}Mg, 87 MeV/u for ^{32}Mg, and 94 MeV/u for ^{31}Na, where they reacted with the secondary ^{9}Be target (376 mg/cm^2). The rate of the secondary beams, for a momentum acceptance of 2%, was $\sim 2 \times 10^4$ pps for ^{31}Mg, $\sim 1 \times 10^4$ pps for ^{32}Mg and $\sim$ 700 pps for ^{31}Na. Gamma rays emitted from the reactions ^{9}Be(^{31}Mg, ^{30}Na + γ)X, ^{9}Be(^{32}Mg, ^{30}Na + γ)X and ^{9}Be(^{31}Na, ^{30}Na + γ)X were detected with SeGA [18], an array of 16 32-fold segmented high-purity germanium detectors. For this measurement SeGA consisted of seven detectors at 37° and nine detectors at 90° surrounding the S800 target position. Outgoing ^{30}Na fragments were identified by energy-loss and time-of-flight measurements in the S800 spectrometer [19].

[4] The term npnh ($n = 0, 1, 2, 3, 4$) denotes the number of particles (np) promoted to the next oscillator shell and the number of holes (nh) that consequently emerge.

[5] A distinction has been made to the terminology used for the different nucleon-removal reactions due to the direct nature of the 1p and 1n reactions. The latter two will be called knockout reactions hereafter.

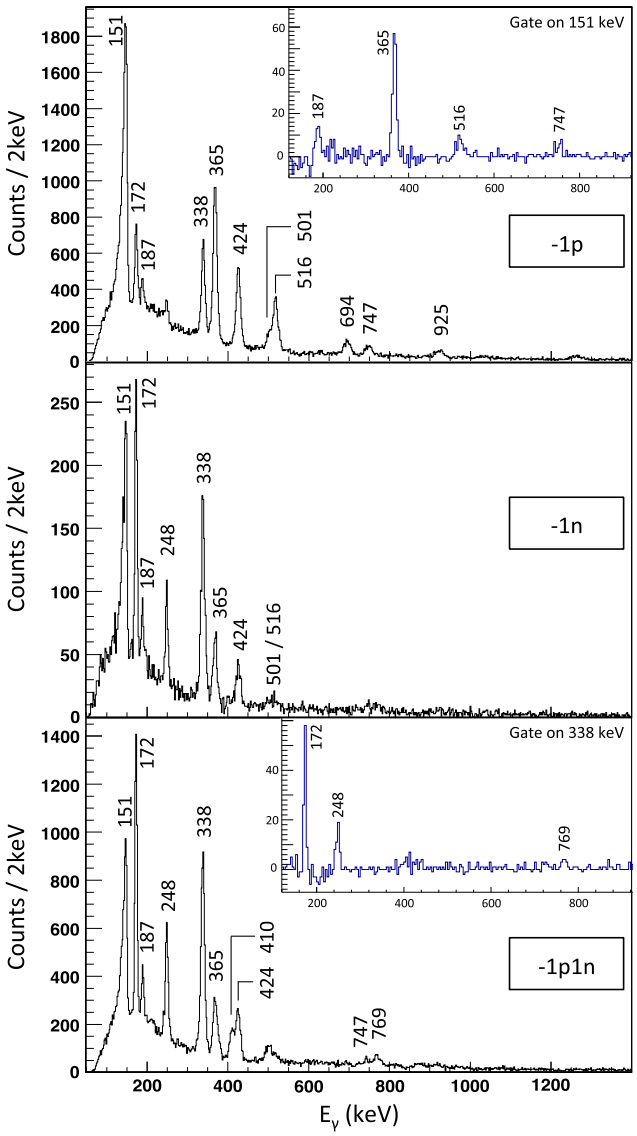

Fig. 1. Doppler-corrected γ-ray spectra from all 16 SeGA detectors in coincidence with ^{30}Na fragments in the (top) ^{9}Be(^{31}Mg, ^{30}Na + γ)X, (middle) ^{9}Be(^{31}Na, ^{30}Na + γ)X and (bottom) ^{9}Be(^{32}Mg, ^{30}Na + γ)X reactions. Selected gated spectra are presented as insets.

3. Results

Doppler-corrected γ-ray spectra in coincidence with ^{30}Na fragments from the three reactions are shown in Fig. 1. These are assigned as γ rays de-exciting excited states in ^{30}Na. The 172(2), 187(2), 248(2), 338(2), 516(2), 694(3), 747(3), 769(3), 1032(3) and 1263(3) keV transitions are observed for the first time. The 365(2) [15], 410(2) [15], 424(2) [13,16,12], 501(2) [16] and 925(3) [16] transitions have already been observed in the corresponding references. A γ ray at 148 keV is also observed, which we associate with the 151(1) keV transition of Ref. [15]. The energy shift is due to the long lifetime of this transition (of the order of 500 ps), evident from its low-energy tail in the γ-ray spectrum.

From a $\gamma - \gamma$ coincidence analysis the observed level scheme of ^{30}Na is deduced in each reaction and shown in Fig. 2. We have identified four distinct structures (bands) based on the different intensities with which these are populated in each reaction.

Band 1: This forms the ground-state band of ^{30}Na. The state at 424 keV has already been established [13,12,14] and assigned to be

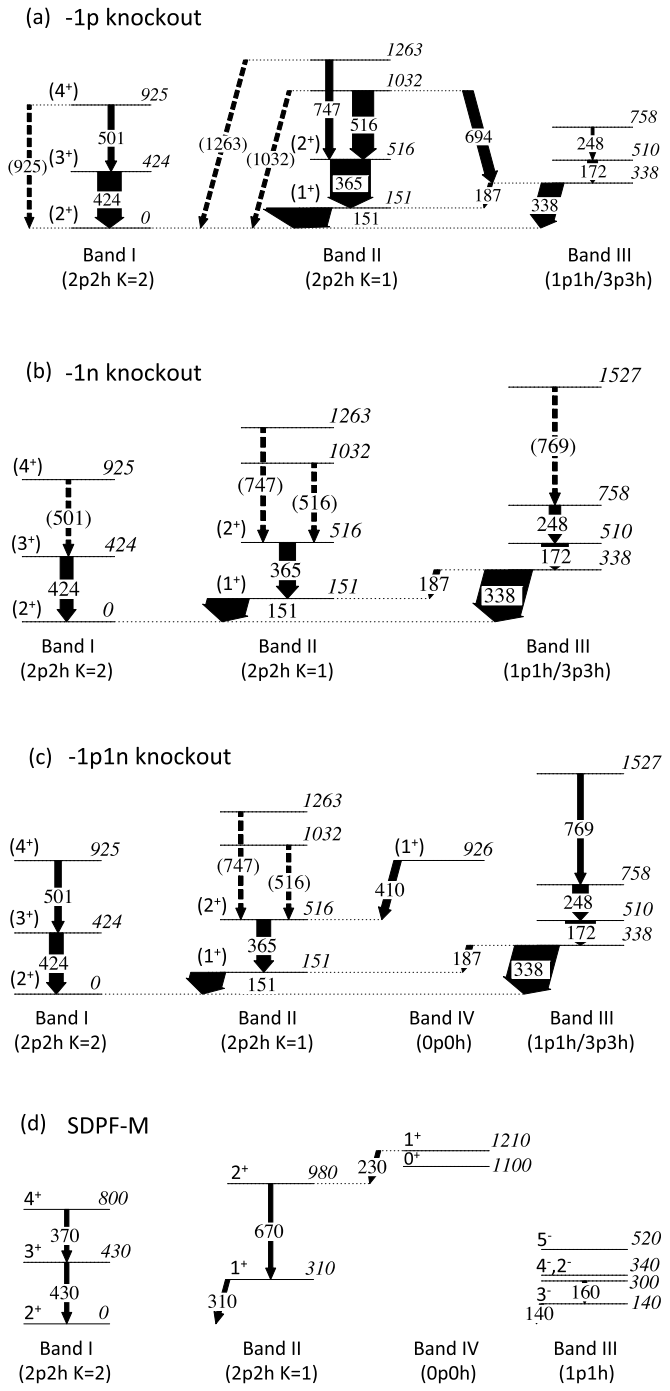

Fig. 2. Level scheme of ^{30}Na deduced by γ–γ coincidence analysis in the (a) 1p knockout reaction, (b) 1n knockout reaction and (c) 1p1n removal reaction. The arrows are proportional to the intensities of the γ rays as measured in the singles spectra. Dotted arrows indicate γ rays observed in the singles spectrum but not in coincidence with other γ rays. In (a) this is because these γ rays are not in coincidence with any other γ ray. In (b) and (c) this is due to the limited statistics of our γ–γ matrix; however, these transitions have been firmly placed in the level scheme from the 1p knockout reaction. Tentative spin assignments (see Section 3) are shown in parentheses. In (d) the calculated levels have been adapted from Ref. [10]. The γ rays are shown for easy comparison between theory and experiment.

the $J = 3$ member of the $K = 2$ rotational band built upon the 2^+ ground state. A clear transition at 501 keV in coincidence with the 424 keV is observed, verifying and supporting the suggestion by Seidlitz *et al.* [16] that this level at 925 keV forms the $J = 4$ member of the ground state rotational band. In the singles spectrum we observe a 925 keV γ ray, which is not in coincidence with any other transition. We assign this γ ray as the one de-exciting the 925 keV level. The experimentally observed branching ratio of the $4_1^+ \rightarrow 2_1^+$ and $4_1^+ \rightarrow 3_1^+$ transitions is 60(8)% and 40(5)%, respectively, yielding smaller uncertainties compared to the one deduced in Ref. [16] (of 67(10)% and 33(10)%).

Band II: The first two transitions (151 and 365 keV) of this band are consistent with the results from the β-decay experiment of Ref. [15], therefore we adopt their spin assignments of 1^+ and 2^+, respectively. The 151 keV level has a long lifetime (of the order of 500 ps) resulting in a de-exciting γ ray with a characteristic tail towards lower energies and a shift in its energy (148 keV). The states at 1032 and 1263 keV are observed for the first time together with their de-exciting γ rays.

Band III: This band has been observed for the first time. It is strongly populated both in the 1p1n removal and in the 1n knockout reactions. These reactions involve removing a neutron from the *sd* and *pf* shells, with the latter leading to the population of negative-parity states. We therefore argue that Band III is of negative parity, see discussion in Section 4.

Band IV: This band has been identified as a separate structure, despite the fact that its level lies very close to the 925 keV level of Band I, since it has been populated only in the 1p1n removal reaction. According to the experiment of Ref. [15], the 410 keV transition belongs to the 0p0h 1^+ state. We believe the reason we populate this state only in the 1p1n reaction is due to the fact that this reaction is not a purely direct two-nucleon knockout reaction. It rather includes evaporation channels, i.e. a neutron evaporates after one-proton removal. Therefore, the decay will also have a statistical character and levels not observed in the direct 1p (^{31}Mg $\rightarrow$ ^{30}Na) and 1n (^{31}Na $\rightarrow$ ^{30}Na) reactions will be populated in this reaction.

4. Discussion

State-of-the art shell model calculations using the SDPF-M interaction, which allow neutron excitations across the $N = 20$ shell gap and reproduce the spectroscopic observables of nuclei in this region, suggest that bands built on 1p1h, 2p2h, 3p3h and 0p0h neutron configurations should coexist at low energies [10]. Here we argue that exploiting the different reaction mechanisms, such configurations can be preferentially and selectively populated and identified. We will only use the 1p and 1n knockout reactions, since our arguments are based on the direct character of the reaction. In a simple picture, the reaction mechanism and the states that are populated in ^{30}Na are shown in Fig. 3.

4.1. Structure assignment

1p knockout (^{31}Mg $\rightarrow$ ^{30}Na): In the ground state of ^{31}Mg, the 12 protons are filling the *sd* shell and two of the 19 neutrons lie in the *pf* shell [20]. The 1p knockout reaction thus will result in populating 2p2h states in ^{30}Na, as is illustrated in Fig. 3(a).

1n knockout (^{31}Na $\rightarrow$ ^{30}Na): The ground state of ^{31}Na may be considered a proton hole coupled to a ^{32}Mg core, where 2p2h and 4p4h configurations dominate its ground state [6]. The 1n knockout thus will result in probing 1p1h, 2p2h, and 3p3h states in ^{30}Na, depending on whether the neutron was knocked out from the *pf* shell in a 2p2h configuration, the *sd* shell in a 2p2h configuration or the *pf* shell in a 4p4h configuration, respectively, as shown in Fig. 3(b). So in this reaction, all 2p2h, 1p1h and 3p3h configurations may be populated.

By analyzing the number of γ rays and the number of ^{30}Na fragments, we were able to establish the strength with which each

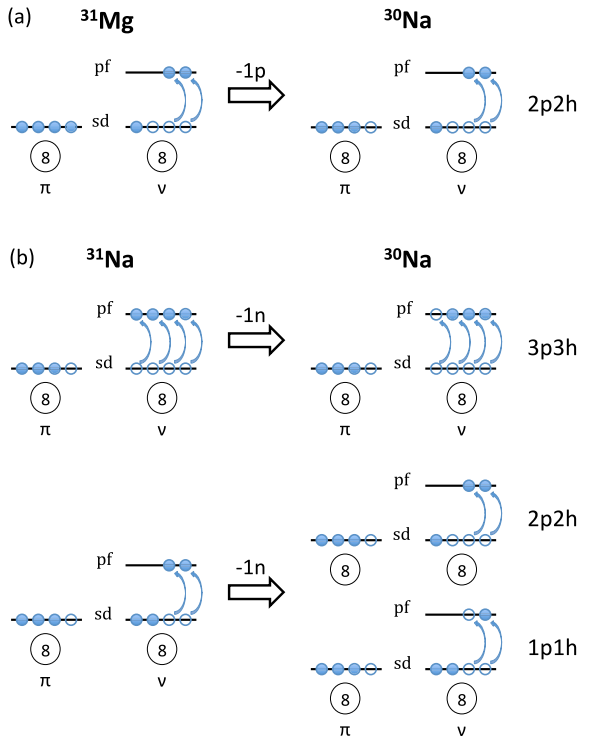

Fig. 3. (Color online.) Sketch of the (a) 1p and (b) 1n knockout reactions and the configurations populated in ^{30}Na. Particles (filled circles) and holes (empty circles) occupy shell model orbitals. (a) In the 1p knockout reaction only 2p2h configurations in ^{30}Na should be populated. (b) Knocking out 1n from ^{31}Na can either populate 3p3h states in ^{30}Na when the neutron is knocked out from a 4p4h ground state in ^{31}Na, or 2p2h and 1p1h configurations when the neutron is knocked out from the ^{31}Na ground state dominated by 2p2h excitations.

Table 1
Intensity of each structure as was populated in the 1p and 1n knockout reactions. The *npn*h configuration is assigned according to the argumentation made in the text. The K assignments are taken from Ref. [10].

Reaction	2p2h ($K=2$) Band I	2p2h ($K=1$) Band II	1p1h/3p3h Band III
^{9}Be(^{31}Mg, ^{30}Na + γ)X	41(6)%	49(6)%	10(2)%
^{9}Be(^{31}Na, ^{30}Na + γ)X	29(7)%	30(5)%	42(6)%

band (I, II, III) is populated in either the 1p or 1n knockout reaction. In the population of Band I, the ground state contribution is also included, i.e. its population comes from the intensity of the 424 and 925 keV γ rays plus the direct population of the ground state.[6] These numbers are shown in Table 1.

In the 1p knockout reaction, Bands I and II take most of the intensity with 90% population. We assign these bands as 2p2h excitations. The lower population of Band III (10%) in the 1p knockout suggests this structure does not have a large 2p2h component. We interpret the small population of this band as being due to side feeding and configuration mixing.

In the 1n knockout reaction the picture is different. Here we strongly populate all three bands, leading us to conclude that Band III corresponds to 1p1h and 3p3h excitations, since we have already assigned Bands I and II as of 2p2h nature. Hence Band III is of negative parity.

[6] The direct ground state population is calculated by subtracting the absolute intensity of the γ rays that feed the ground state from the total number of ^{30}Na fragments.

4.2. Comparison to shell model predictions

The theoretical predictions in this region depend strongly on the effective interaction. The current experimental results with the observation of a rather complete set of coexisting configurations provide an important test for the theoretical predictions.

Here, we compare our experimental findings with the calculations of Ref. [10], as this is the last published theoretical calculations regarding this odd–odd nucleus. Nevertheless, the present experimental work will serve as an invaluable reference for future theoretical calculations and their refinement.

Utsuno et al. [10] predict the co-existence of different particle–hole configurations and we confirm this experimentally; Bands I, II, III and IV have been assigned as being of 2p2h, 2p2h, 1p1h/3p3h and 0p0h nature, respectively. Our assignment of a dominant 1p1h/3p3h configuration to Band III provides the first evidence for the location of the negative parity states in this key ("transitional") nucleus.

As shown in Fig. 6(d) of Ref. [10], the relative excitations between the various particle–hole configurations and specifically that separating the 2p2h and 1p1h configurations can constrain the *sd*–*pf* shell gap. The measured excitation energy of 338 keV for the 1p1h/3p3h band (Band III) above the 2p2h ground state (Band I) is close to the calculated value in Ref. [10] of ∼140 keV. Our data provides important confirmation of the calculation, supporting the notion of a reduced *sd*–*pf* shell gap (3.3 MeV) at $N=19$.

While likely within expected uncertainties for shell model calculations, when comparing the measured level energies (Fig. 2(a)–(c)) with the calculated ones (Fig. 2(d)), we find systematically an overestimation of the level energy for the positive-parity states by a few 100 keV, while the negative-parity states are lower in energy than what is observed in the present experiment. It is interesting to speculate whether these systematic differences reflect a further reduction in the *sd*–*pf* shell gap and can then help refine the effective interactions used in these shell model calculations.

5. Summary

We have studied the odd–odd nucleus ^{30}Na via three different nucleon-removal reactions, which allowed us to identify multiple *npn*h configurations, co-existing at low energies. The relative excitation of each configuration constrains the *sd*–*pf* shell gap at $N=19$ and helps refine the phenomenological interactions used in this region of the nuclear chart.

Acknowledgements

This work was supported by DOE contract No. DE-AC02-05CH11231, by the National Science Foundation under Grant PHY-1102511 and by the Helmholtz International Center for FAIR within the framework of the LOEWE program (Landesoffensive zur Entwicklung Wissenschaftlich-Ökonomischer Exzellenz) launched by the State of Hesse. M.P. acknowledges Alfredo Poves and Takaharu Otsuka for fruitful discussions.

References

[1] O. Sorlin, M.-G. Porquet, Nuclear magic numbers: new features far from stability, Prog. Part. Nucl. Phys. 61 (2) (2008) 602–673, http://dx.doi.org/10.1016/j.ppnp.2008.05.001, http://www.sciencedirect.com/science/article/pii/S0146641008000380.

[2] C. Thibault, R. Klapisch, C. Rigaud, A.M. Poskanzer, R. Prieels, L. Lessard, W. Reisdorf, Direct measurement of the masses of ^{11}Li and $^{26-32}$Na with an on-line mass spectrometer, Phys. Rev. C 12 (1975) 644–657, http://dx.doi.org/10.1103/PhysRevC.12.644.

[3] X. Campi, H. Flocard, A. Kerman, S. Koonin, Shape transition in the neutron rich sodium isotopes, Nucl. Phys. A 251 (2) (1975) 193–205, http://dx.doi.org/10.1016/0375-9474(75)90065-2.

[4] A. Poves, J. Retamosa, The onset of deformation at the $N = 20$ neutron shell closure far from stability, Phys. Lett. B 184 (4) (1987) 311–315, http://dx.doi.org/10.1016/0370-2693(87)90171-7, http://www.sciencedirect.com/science/article/pii/0370269387901717.

[5] E.K. Warburton, J.A. Becker, B.A. Brown, Mass systematics for $A = 29$–44 nuclei: the deformed $A \sim 32$ region, Phys. Rev. C 41 (1990) 1147–1166, http://dx.doi.org/10.1103/PhysRevC.41.1147.

[6] E. Caurier, F. Nowacki, A. Poves, Merging of the islands of inversion at $N = 20$ and $N = 28$, Phys. Rev. C 90 (2014) 014302, http://dx.doi.org/10.1103/PhysRevC.90.014302.

[7] T. Otsuka, T. Suzuki, M. Honma, Y. Utsuno, N. Tsunoda, K. Tsukiyama, M. Hjorth-Jensen, Novel features of nuclear forces and shell evolution in exotic nuclei, Phys. Rev. Lett. 104 (2010) 012501, http://dx.doi.org/10.1103/PhysRevLett.104.012501.

[8] T. Otsuka, T. Suzuki, R. Fujimoto, H. Grawe, Y. Akaishi, Evolution of nuclear shells due to the tensor force, Phys. Rev. Lett. 95 (2005) 232502, http://dx.doi.org/10.1103/PhysRevLett.95.232502.

[9] Y. Utsuno, T. Otsuka, T. Mizusaki, M. Honma, Varying shell gap and deformation in $N \sim 20$ unstable nuclei studied by the Monte Carlo shell model, Phys. Rev. C 60 (1999) 054315, http://dx.doi.org/10.1103/PhysRevC.60.054315.

[10] Y. Utsuno, T. Otsuka, T. Glasmacher, T. Mizusaki, M. Honma, Onset of intruder ground state in exotic Na isotopes and evolution of the $n = 20$ shell gap, Phys. Rev. C 70 (2004) 044307, http://dx.doi.org/10.1103/PhysRevC.70.044307.

[11] G. Huber, F. Touchard, S. Büttgenbach, C. Thibault, R. Klapisch, H.T. Duong, S. Liberman, J. Pinard, J.L. Vialle, P. Juncar, P. Jacquinot, Spins, magnetic moments, and isotope shifts of $^{21-31}$Na by high resolution laser spectroscopy of the atomic D_1 line, Phys. Rev. C 18 (1978) 2342–2354, http://dx.doi.org/10.1103/PhysRevC.18.2342.

[12] B.V. Pritychenko, T. Glasmacher, P.D. Cottle, R.W. Ibbotson, K.W. Kemper, K.L. Miller, L.A. Riley, H. Scheit, Transition to the "island of inversion": fast-beam γ-ray spectroscopy of ^{28,30}Na, Phys. Rev. C 66 (2002) 024325, http://dx.doi.org/10.1103/PhysRevC.66.024325.

[13] S. Ettenauer, H. Zwahlen, P. Adrich, D. Bazin, C.M. Campbell, J.M. Cook, A.D. Davies, D.-C. Dinca, A. Gade, T. Glasmacher, J.-L. Lecouey, W.F. Mueller, T. Otsuka, R.R. Reynolds, L.A. Riley, J.R. Terry, Y. Utsuno, K. Yoneda, Intermediate-energy Coulomb excitation of ^{30}Na, Phys. Rev. C 78 (2008) 017302, http://dx.doi.org/10.1103/PhysRevC.78.017302.

[14] Z. Elekes, Z. Dombrádi, A. Saito, N. Aoi, H. Baba, K. Demichi, Z. Fülöp, J. Gibelin, T. Gomi, H. Hasegawa, N. Imai, M. Ishihara, H. Iwasaki, S. Kanno, S. Kawai, T. Kishida, T. Kubo, K. Kurita, Y. Matsuyama, S. Michimasa, T. Minemura, T. Motobayashi, M. Notani, T. Ohnishi, H.J. Ong, S. Ota, A. Ozawa, H.K. Sakai, H. Sakurai, S. Shimoura, E. Takeshita, S. Takeuchi, M. Tamaki, Y. Togano, K. Yamada, Y. Yanagisawa, K. Yoneda, Proton inelastic scattering studies at the borders of the "island of inversion": the ^{30,31}Na and ^{33,34}Mg case, Phys. Rev. C 73 (2006) 044314, http://dx.doi.org/10.1103/PhysRevC.73.044314.

[15] V. Tripathi, S.L. Tabor, P.F. Mantica, Y. Utsuno, P. Bender, J. Cook, C.R. Hoffman, S. Lee, T. Otsuka, J. Pereira, M. Perry, K. Pepper, J.S. Pinter, J. Stoker, A. Volya, D. Weisshaar, Competition between normal and intruder states inside the "island of inversion", Phys. Rev. C 76 (2007) 021301, http://dx.doi.org/10.1103/PhysRevC.76.021301.

[16] M. Seidlitz, P. Reiter, R. Altenkirch, B. Bastin, C. Bauer, A. Blazhev, N. Bree, B. Bruyneel, P.A. Butler, J. Cederkäll, T. Davinson, H. De Witte, D.D. DiJulio, J. Diriken, L.P. Gaffney, K. Geibel, G. Georgiev, R. Gernhäuser, M. Huyse, N. Kesteloot, T. Kröll, R. Krücken, R. Lutter, J. Pakarinen, F. Radeck, M. Scheck, D. Schneiders, B. Siebeck, C. Sotty, T. Steinbach, J. Taprogge, P. Van Duppen, J. Van de Walle, D. Voulot, N. Warr, F. Wenander, K. Wimmer, P.J. Woods, K. Wrzosek-Lipska, Coulomb excitation of ^{29,30}Na: mapping the borders of the island of inversion, Phys. Rev. C 89 (2014) 024309, http://dx.doi.org/10.1103/PhysRevC.89.024309.

[17] D. Morrissey, B. Sherrill, M. Steiner, A. Stolz, I. Wiedenhoever, Commissioning the A1900 projectile fragment separator, in: 14th International Conference on Electromagnetic Isotope Separators and Techniques Related to Their Applications, Nucl. Instrum. Methods Phys. Res., Sect. B, Beam Interact. Mater. Atoms 204 (0) (2003) 90–96, http://dx.doi.org/10.1016/S0168-583X(02)01895-5.

[18] W. Mueller, J. Church, T. Glasmacher, D. Gutknecht, G. Hackman, P. Hansen, Z. Hu, K. Miller, P. Quirin, Thirty-two-fold segmented germanium detectors to identify γ-rays from intermediate-energy exotic beams, Nucl. Instrum. Methods Phys. Res., Sect. A, Accel. Spectrom. Detect. Assoc. Equip. 466 (3) (2001) 492–498, http://dx.doi.org/10.1016/S0168-9002(01)00257-1.

[19] D. Bazin, J. Caggiano, B. Sherrill, J. Yurkon, A. Zeller, The S800 spectrograph, in: 14th International Conference on Electromagnetic Isotope Separators and Techniques Related to Their Applications, Nucl. Instrum. Methods Phys. Res., Sect. B, Beam Interact. Mater. Atoms 204 (2003) 629–633, http://dx.doi.org/10.1016/S0168-583X(02)02142-0.

[20] G. Neyens, M. Kowalska, D. Yordanov, K. Blaum, P. Himpe, P. Lievens, S. Mallion, R. Neugart, N. Vermeulen, Y. Utsuno, T. Otsuka, Measurement of the spin and magnetic moment of ^{31}Mg: evidence for a strongly deformed intruder ground state, Phys. Rev. Lett. 94 (2005) 022501, http://dx.doi.org/10.1103/PhysRevLett.94.022501.